BENCHMARKING OF NATURAL SCENE IMAGE DATASET IN DEGRADED CONDITIONS FOR VISIBILITY ENHANCEMENT

[1,]Sourav Dey Roy, [2,*]Tannistha Pal, and [1,#]Mrinal Kanti Bhowmik*

[1]Department of Computer Science and Engineering, Tripura University (A Central University), Suryamaninagar-799022, Tripura (W), India

[2]Department of Computer Science and Engineering, National Institute of Technology Agartala, Jirania-799046, Tripura (W), India

2021 IEEE International Conference on Image Processing (ICIP) | 978-1-6654-4115-5/21/$31.00 ©2021 IEEE | DOI: 10.1109/ICIP42928.2021.9506573

ABSTRACT

Poor visibility due to existence of fog and other associated particles in the atmosphere is the most fundamental problem for current vision applications. Recently, techniques for visibility enhancement of images have received a significant attention. However, validation of the existing techniques remains scare due to the lack of balanced distribution on the existing datasets. In this paper, a newly designed dataset entitled "SAMEER-TU Outdoor Dataset" is proposed. The dataset contains 5880 images of urban scenes in fog, poor illumination and clear conditions. Also, ground truths are provided in terms of meteorological weather parameters and corresponding clear scene images of the degraded images. On the designed dataset, quantitative analysis of existing visibility enhancement techniques (i.e., conventional and deep learning techniques) are performed based on qualitative evaluation metrics. It comes as no surprise that the existing visibility enhancement techniques and there still existing significant for further improvement.

Index Terms— Atmospheric Conditions; SAMEER-TU Outdoor Dataset; Visibility Enhancement; Quantitative Analysis.

1. INTRODUCTION

Many of the machine vision systems including surveillance, traffic control, virtual reality, vehicle navigation, etc. are actually configured to operate under clear visibility, but this does not happen all the time. In outdoor scenarios, due to the presence of aerosol and other related particles in the direction, the light transmitted from the target is dispersed in the atmosphere. Because of its effect, the captured images mostly suffer from low contrast, faint colour, and reduced visibility, thus decreases the efficiency of high-level computer vision tasks. In real world situations, adverse atmospheric/ weather patterns can have a major effect on traffic in urban areas, thus reducing the coefficient of friction on highways, which can cause traffic congestion and severe traffic accidents, with a great potential to be dangerous [1]. Therefore, noticeable attention has been paid to the development of computer-aided video and image enhancement algorithms for a wide variety of applications, including civil and military areas, such as remote sensing, object detection and traffic monitoring [1]. Conversely, understanding the atmospheric/ weather conditions on scene appearance seems easy task for human visual system i.e., to tell whether a given image is fog, clear day or other degraded conditions which in turns out to be challenging task for computer vision systems.

During the last decades, numerous algorithms has been reported in the literature for visibility enhancement based on single and multiple image approaches [2]. The substantial advancement of complex visibility enhancement algorithms instigates from the availability of benchmark datasets that offers a balanced coverage of the representative atmospheric and weather challenges. Many benchmark datasets are designed in the literature to meet the growing demands of designing and benchmarking modern visibility enhancement algorithms [1][3]-[9].

The key highlights of the characteristics associated with each available dataset adopted by most researchers for qualitative benchmarking of the visibility algorithms and comparison of our newly designed dataset are displayed in Table 1. Even though the available datasets (so as reviewed in Table 1) have advanced the research for visibility enhancement but each of these datasets have certain drawbacks. As found in the literature, most of the available datasets [1][3]-[9] as reviewed in Table 1 contains visual images of outdoor/ indoor scenes degraded by haze condition. On the otherhand, though FRIDA [8] dataset contains visual images in fog degraded conditions but all the images of FRIDA dataset [8] are synthetically generated where fogs are added artificially on the scenes. Equally, although WILD dataset [9] contains visual images of real-world scenes degraded due to fog condition but these datasets are restricted in scale to benchmark any visibility enhancement algorithms.

Depending upon the significance of visibility enhancement for computer vision applications, the primary contributions are summarized below:

1. We describe the designing issues of a newly created "Society of Applied Microwave Electronics Engineering & Research-Tripura University (SAMEER-TU) Outdoor Dataset" so that the researchers can use this dataset for testing and ranking the existing state-of-the-art and new algorithms/ models for visibility enhancement in degraded atmospheric conditions. The dataset contains 5880 images in degraded complex scenarios including for, poor illumination and clear conditions. Along with the dataset, meteorological weather information associated on the capturing day of the dataset are provided with the dataset.
2. With the designed dataset, we provide a qualitative and quantitative comparison of sixteen state-of-the-art visibility enhancement techniques (including traditional and deep learning techniques based on metrics of quality evaluation based on reference and no reference image) and thus provide detailed insights into the strengths and shortcomings of current visibility enhancement algorithms for atmospheric/ weather degraded scenes restoration.

Paper Outline. In Section 2, elaborate description related to the collection and creation of SAMEER-TU Outdoor dataset in degraded conditions are provided. Section 3 compares and contrast the conventional and deep learning based techniques for restoration of weather degraded images on the designed dataset are provided. And finally, the paper concludes with Section 4.

2. SAMEER-TU OUTDOOR DATASET IN DEGRADED CONDITIONS

The appearance of an outdoor scene is extremely tangled due to the existence different atmospheric and weather conditions. To meet up the specific necessities, we proposed a new dataset entitled as "Society of Applied Microwave Electronics Engineering & Research-Tripura University (SAMEER-TU) Outdoor Dataset" under degraded

*Both the first and second authors have equally contributed in this manuscript.
#Corresponding Author (E-mail: mrinalkantibhowmik@tripurauniv.in).

Table 1: Overview of Previous Datasets for Qualitative Benchmarking of Visibility Enhancement Techniques

Name of the Dataset		Year of Release	Weather Conditions	Total No. of Images	Resolution	Type of Dataset	Format	Camera Model	Ground Truth Information	Accessibility
NH-Haze	[3]	2020	H/CS	110	[5456×3632]	VI	.jpg	Sony A5000	CS	A
O-Haze	[4]	2018	H/CS	90	[5456×3632]	VI	.jpg	Sony A5000	CS	A
I-Haze	[5]	2018	H/CS	70	[5456×3632]	VI	.jpg	Sony A5000	CS	A
RESIDE-β/ RESIDE-S	[1]	2018	H/ CS	90967	[178×178] to [620×460]	VI	.jpg	NP	BBO	A
HazeRD	[6]	2017	H/CS	28	[3888×2592] to [3873×2516]	VI	.jpg	NP	DI/CS	A
D-HAZY	[7]	2016	H/CS	1400	[150×96]	VI	.jpg	NP	DI/CS	A
FRIDA/FRIDA-2	[8]	2010/2012	F/CS	410	[640×480]	VI	.jpg	NP	CS	A
WILD	[9]	2002	M/R/H/F/CL/CS	831	[1520×1008]	VI	.jpg	Kodak DCS 315	DI/MI	A
SAMEER-TU Outdoor Dataset [Our Dataset]			F/PI/CS	5880	[1920×1080] to [640×480]	VI/II	.jpg	Nikon D5100; FLIR E60	MI/CS	A

F- Fog; H- Haze; R- Rain; M- Mist; PI- Poor Illumination; CS- Clear Scene; CL- Cloud; VI- Visual Imaging; II- Infrared Imaging; MI- Meteorological Information; BBO- Bounding Box based Objects; RESIDE-S- Reside Standard; DI- Depth Image; NP- Not Provided; A- Available Dataset

Table 2: Distribution of SAMEER-TU Outdoor Dataset in Degraded Conditions

Atmospheric/ Weather Conditions	Image Modality		Total Number of Images
	Visual Camera (Camera Model: Nikon D5100)	Infrared Camera (Camera Model: FLIR E60)	
	VI	II	
Fog Condition	1020	40	40	1100
Poor Illumination Condition	250	28	28	306
Clear Condition	4370	52	52	4474
Total Number of Images	**5640**	**120**	**120**	**5880**

VI- Visual Imaging; II- Infrared Imaging

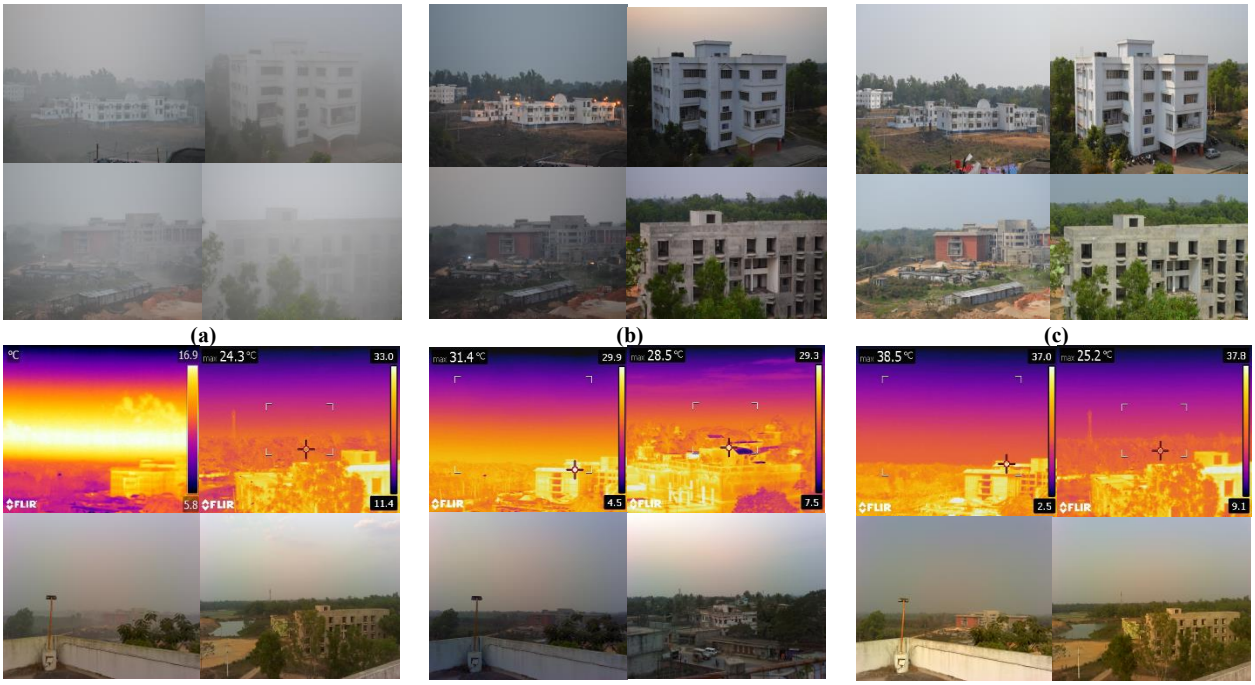

Fig. 1. Sample Frames of SAMEER-TU Outdoor Dataset: (a), (b), (c) Visual Images in Fog, Poor Illumination and Clear Condition Respectively Captured Using Nikon D5100 Visual Camera; (d), (e), (f) Infrared Images and Its Corresponding Visual Images in Fog, Poor Illumination and Clear Condition Respectively Captured Using FLIR E60 Infrared Camera

atmospheric and weather conditions. In this section, designing issues, dataset statistics, naming convention, and contributive features of the SAMEER-TU Outdoor dataset are presented.

2.1. Designing Concerns and Capturing Conditions

The images in SAMEER-TU Outdoor Dataset are taken in weather and illumination effects. For designing the dataset, we collected two modalities of images including visual images and infrared images in each of the considered capturing conditions. In general, low visibility due to fog and other related condition happens when the difference between the average temperature and the dew point is less than 2.5^{O}C and visibility is less than 1 KM [10]. On the basis of these observations, several factors are considered during the data capturing so as to maintain the uniformity and decrease the negative impact on analysis. The first factor is the capturing conditions. In this dataset, we have considered three atmospheric/ weather conditions including foggy condition, poor illumination condition and clear condition. The second component is the camera specification. In designing our dataset, we captured the visual images using Nikon D5100 visual camera with 18-55 mm focal length of lens, 1/125-1/200 shutter speed, and f/5.6-f/8 aperture range. The spatial resolution of the visual images is 4928×3264 pixels. On the otherhand, infrared images are captured using FLIR E60 infrared camera with a thermal sensitivity of 0.05°C and a -20 to 650°C (-4 to 1202°F) temperature range. Along with the infrared images, corresponding visual images in each of the specific conditions of the dataset are also present. The resolution of the infrared images and their corresponding visual images is 320×240 pixels. Each of the used cameras are mounted over a tripod stand which is placed rigidly to a

Table 3: Naming Convention of SAMEER-TU Outdoor Dataset

Atmospheric Condition		Camera Modality		Natural Scenes		Capturing Day	
Condition	Codes	Modality	Codes	Scene	Codes	Day	Codes
Fog	F	Visual Camera	VC	Natural Scene 1	NS1	Day1	D1
Poor Illumination	PI	Infrared Camera	IC	…	…	...	...
Clear Condition	CC			Natural Scene n	NSn	Dayn	Dn

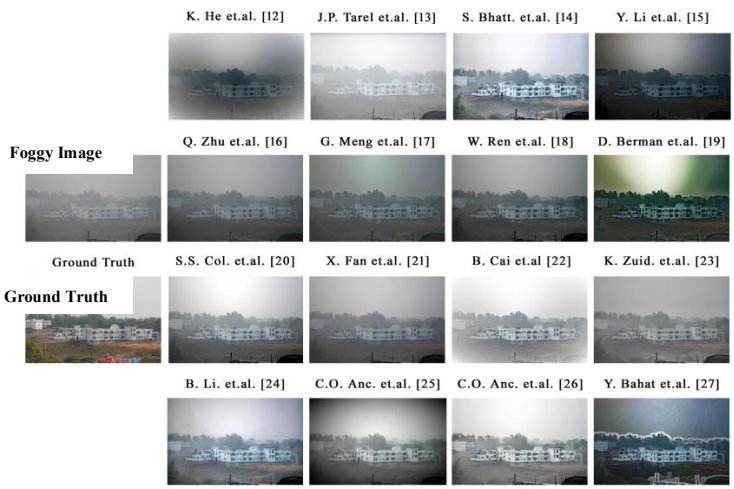

Fig. 2. Visual Results of the Representative Visibility Enhancement Techniques

weather-proof glass room of 4 ft. ×4 ft. The second factor is the outdoor environment condition. During acquisition, the temperature, humidity, dew point, wind speed, and visibility varies from 10°C to 24°C, 95% to 100%, 10°C to 15°C, 1mph to 3.5 mph, and 0 KM to 1 KM respectively. All the images of the SAMEER-TU Outdoor dataset are captured for the whole day from 6 AM to 6 PM in the outdoor environment after a 15-minute period in the alternate five days during the months of winter season in Tripura, India.

2.2. Dataset Statistics and Naming Convention

Using the above mentioned acquisition procedure, the total distribution of acquired images of the created dataset in each of the considered conditions is tabulated in Table 2. In this dataset, there are total 5880 images of outdoor scenes. The dataset comprises of 1100 images in fog condition, 306 images in poor illumination condition, and 4474 images in clear condition. Some of the exemplar images from SAMEER-TU Outdoor Dataset representing different captured conditions are shown in Fig. 1.

After acquisition, every images of the dataset are named for understanding its category during the analysis. For meaningful naming of the images, certain codes are used as shown in Table 3. The naming code for the images of the created dataset is represented as: Atmospheric-Condition_ Natural-Scene-Number_Capturing-Day_Image-ID.jpg. By using of the above naming convention, every image in the dataset acquires a distinctive identity. For example, from the image name F_NS1_D1_VC_I(1).jpg, it is clear that the image with ID I(1) is fog degraded (F) image of natural scene 1 (NS1) acquired in Day 1 using visual camera (VC).

2.3. Ground Truth Information

Ground truth information is one of significant information required for qualitative benchmarking of new algorithms/ models. Along with the dataset, two useful ground truth information are provided. Firstly, with each of the visibility degraded images in fog and poor illumination conditions, corresponding images in clear condition are also provided as a ground truth with the dataset. Secondly, each images of the dataset are tagged with useful meteorological information i.e., temperature (°C), humidity (%), dew point (°C), wind speed (kilometre per hour), direction of wind, visibility (KM), and atmospheric pressure (mbar) so as attained from Regional Meteorological Department of Tripura.

2.4. Contributive Features of the Dataset

The primary contributive features of the designed dataset are summarized below:

1. The dataset consists of **images (i.e., both visual and infrared images) in fog, poor illumination, and clear conditions** acquired from different regions of Tripura. The images in fog conditions are basically random combination of slight, medium and dense fog.
2. The images of the dataset are urban scenes which, due to the presence of many candidate objects such as cars, pedestrians, animals, homes, office buildings, trees, streets, and people, correlate to greater surface differences.
3. For all the degraded images in fog and poor illumination conditions, **corresponding clear scene images are provided** so that the researches can use these images **as ground truth images** so that the researchers can verify the effectiveness of the models for visibility enhancement.
4. Moreover, **ground truth information** corresponding to each images of the dataset are provided with the dataset in terms of different variables of earth's atmosphere.

The aforementioned contributive features of the SAMEER-TU Outdoor dataset will be a great help to the computer vision communities as they will be able to test the performance of the developed algorithms on this dataset and compare with such other algorithms. **The dataset is available for the research community on request for non-commercial use in [11].**

3. QUALITATIVE AND QUANTITATIVE ANALYSIS OF FOG DEGRADED IMAGES USING THE STATE-OF-THE-ART METHODS

Visibility enhancement of images degraded due to atmospheric and weather images has received a significant improvement in the past decades. Each of the representative techniques proposed in the literature are either multiple image based approach or single image based approach [2]. The visibility enhancement techniques depending on a single image have received a significant attention in recent years. Since concentration of the atmospheric particles responsible for degradation is different from place to place therefore image dehazing is thus a complex task. In this section, performance of the state-of-the-art visibility enhancement algorithms have been reported for quality restoration of fog degraded images from SAMEER-TU Outdoor Dataset.

Table 4: Qualitative Comparison of the State-of-the-Art Visibility Enhancement Algorithms on SAMEER-TU Outdoor Dataset Using Reference Image Based Quality Assessment Metrics

Visibility Enhancement Methods		Approach/ Technique	Quality Assessment Metrics MSE (↓)	PSNR (↑)	NCC (↓)	MD (↓)	AD (↓)	SC (↓)	NAE (↓)
K. He et.al.	[12]	SI/ DCPT	4948.64±1567.53	11.18±0.06	1.44±0.15	201.63±16.23	45.73±15.64	1.42±0.02	0.51±0.21
J.P. Tarel et.al.	[13]	SI/ FIBT	3092.62±1325.65	14.21±2.64	0.79±0.01	178.00±5.65	29.49±22.65	0.74±0.26	0.31±0.01
S. Bhattacharya et.al.	[14]	SI/ FIBT	**1235.95±310.58**	**17.37±1.27**	**0.79±0.11**	**106.55±19.48**	**14.73±17.41**	**0.35±0.23**	**0.29±0.07**
Y. Li et.al.	[15]	SI/ FIBT	3960.11±2096.24	12.81±2.49	1.34±0.18	97.83±29.58	31.15±27.13	**1.43±0.20**	0.38±0.13
Q. Zhu et.al.	[16]	SI/ DCPT	2249.81±2246.91	14.21±0.01	0.88±0.16	161.89±44.63	39.86±20.74	0.56±0.17	0.50±0.34
G. Meng et.al.	[17]	SI/ FIBT	2804.21±1489.63	16.33±1.48	1.13±0.14	**134.55**±31.20	**36.33±11.45**	0.76±0.18	0.29±0.06
W.Ren et.al.	[18]	SI/ DLT	3404.47±1035.64	13.77 ±1.06	1.20±0.10	154.54±20.54	32.49±0.95	0.53±0.16	0.45±013
D. Berman et.al.	[19]	SI/ FIBT	3960.68±1795.14	12.96±2.10	1.11±0.15	174.76±22.19	30.75±21.62	0.70±0.20	0.53±0.19
S.S. Colores et.al.	[20]	SI/ LBT	4532.67±1332.85	12.45±1.32	1.37±0.34	189.42±25.73	46.87±20.39	1.58±0.53	0.73±0.13
X. Fan et.al.	[21]	SI/ FIBT	3065.01±1103.87	14.43±2.06	1.31±0.21	181.53±21.31	24.36±15.65	1.12±0.32	0.45±0.15
B. Cai et.al.	[22]	SI/ DLT	3217.45±1265.65	13.63±1.89	1.10±0.15	178.75±31.09	32.45±16.53	1.14±0.21	0.43±0.13
G. Yadav et.al.	[23]	SI/ HIBT	3243.56±1120.12	13.66±2.01	1.00±0.06	181.83±29.10	19.95±1.38	0.95±0.12	0.33±0.08
B. Li. et.al.	[24]	SI/ DLT	**1586.26±582.06**	**16.39±1.78**	**0.79±0.12**	**122.92±20.89**	**12.57±5.79**	**0.49±0.13**	**0.20±0.04**
C.O. Ancuti et.al.	[25]	SI/ FBT	3333.66±1630.99	13.47±2.31	1.32±0.14	154.25±16.88	26.34±22.79	1.24±0.47	0.32±0.02
C.O. Ancuti et.al.	[26]	SI/ FBT	2105.08±1424.57	14.96±0.84	0.93±0.07	123.50±11.08	24.64±24.69	1.04±0.16	0.31±0.07
Y. Bahat et.al.	[27]	SI/ FBM	*7510.94±3428.68*	*9.78±1.89*	*1.89±0.85*	*204.67±16.42*	*74.32±24.69*	*1.56±0.48*	*1.58±0.96*

SI- Single Image Enhancement Approach, DCPT- Dark Channel Prior Based Technique; FIBT- Filtering Based Technique; FBT- Fusion Based Technique; DLT- Deep Learning Based Technique; DCPT- Dark Channel Prior Based Technique; LBT- Learning Based Technique; HIBT- Histogram Based Technique; MSE- Mean Square Error; PSNR- Peak Signal to Noise Ratio; NCC- Normalized Cross Correlation; MD- Maximum Difference; AD- Average Difference; SC- Structural Constraint; NAE- Normalized Absolute Error; ↓- Lower Values designates Better Performance; ↑- Higher Values designates Better Performance; Bold Face and Underlined- Best Performed Method; Bold Face- Second Most Best Performed Method; Italics and Underline- Worst Performed Method

Table 5: Qualitative Comparison of the State-of-the-Art Visibility Enhancement Algorithms on SAMEER-TU Outdoor Dataset Using No-Reference Image Based Quality Assessment Metrics

Visibility Enhancement Methods		Approach/ Technique	Quality Assessment Metrics e (↑)	r (↑)	σ (↓)	D (↓)
K. He et.al.	[12]	SI/ DCPT	0.11±0.03	1.02±0.09	*0.79±0.01*	0.74±0.20
J.P. Tarel et.al.	[13]	SI/ FIBT	0.36±0.13	1.45±0.40	0.48±0.16	0.53±0.12
S. Bhattacharya et.al.	[14]	SI/ FIBT	**0.54±0.23**	**2.54±0.87**	**0.32±0.12**	**0.35±1.02**
Y. Li et.al.	[15]	SI/ FIBT	0.25±0.10	1.32±0.65	0.61±0.28	0.68±0.18
Q. Zhu et.al.	[16]	SI/ DCPT	0.36±0.14	1.40±0.53	0.50±0.06	0.51±0.14
G. Meng et.al.	[17]	SI/ FIBT	0.31±0.10	1.38±0.34	0.51±0.18	0.54±0.25
W.Ren et.al.	[18]	SI/ DLT	0.33±0.12	1.38±0.08	0.49±0.16	0.52±0.11
D. Berman et.al.	[19]	SI/ FIBT	0.22±0.14	1.25±0.45	0.65±0.37	0.66±0.22
S.S. Colores et.al.	[20]	SI/ LBT	0.44±0.19	1.66±0.57	0.50±0.12	0.47±0.14
X. Fan et.al.	[21]	SI/ FIBT	0.43±0.11	1.69±0.20	0.52±0.13	0.45±0.23
B. Cai et.al.	[22]	SI/ DLT	0.35±0.19	1.49±0.28	0.59±0.08	0.55±0.17
G. Yadav et.al.	[23]	SI/ HIBT	0.40±0.10	1.61±0.33	0.51±0.10	0.51±0.13
B. Li. et.al.	[24]	SI/ DLT	**0.48±0.20**	**1.82±0.25**	**0.43±0.14**	**0.38±0.08**
C.O. Ancuti et.al.	[25]	SI/ FBT	0.20±0.09	1.08±0.76	0.70±0.18	0.76±0.31
C.O. Ancuti et.al.	[26]	SI/ FBT	0.33±0.10	1.87±0.25	0.56±0.09	0.57±0.16
Y. Bahat et.al.	[27]	SI/ FBM	*0.10±0.05*	*0.95±0.21*	0.72±0.18	*0.81±0.33*

SI- Single Image Enhancement Approach, DCPT- Dark Channel Prior Based Technique; FIBT- Filtering Based Technique; FBT- Fusion Based Technique; DLT- Deep Learning Based Technique; DCPT- Dark Channel Prior Based Technique; LBT- Learning Based Technique; HIBT- Histogram Based Technique; e- Rate of New Visible Edges; r- Mean Ratio; σ- Percentage of Saturated Pixels; D- Perceptual Fog Density; ↓- Lower Values designates Better Performance; ↑- Higher Values designates Better Performance; Bold and Underlined- Best Performed Method; Bold - Second Most Best Performed Method; Italics and Underline- Worst Performed Method

From the literature, sixteen well-known single image based visibility enhancement techniques (i.e., conventional and deep learning based methods) are used. The used methods are: K. He et.al.[130], J.P. Tarel et.al. [13], S. Bhattacharya et.al. [14] Y. Li et.al. [15], Q. Zhu et.al. [16], G. Meng et.al. [17], W.Ren et.al. [18], D. Berman et.al. [19], S.S. Colores et.al. [20] X. Fan et.al. [21], B. Cai et.al. [22], G. Yadav et.al. [23], B. Li. et.al. [24], C.O. Ancuti et.al. [25], C.O. Ancuti et.al. [26], and Y. Bahat et.al. [27]. The associated parameters of each of these used techniques are kept same as mentioned by the respective authors or when not available are adjusted to enhance the results. Fig. 2 displays the visual results of each of the methods tested on SAMEER-TU Outdoor Dataset.

To perform the experiments, 1000 images are used from SAMEER-TU Outdoor Dataset degraded by fog condition (i.e., containing slight, medium and dense fog). Each of the aforementioned techniques are implemented and tested on CPU based Dell Precision Tower 5810 workstation with 64 GB installed memory (RAM). For quantitative comparison, we have used both reference [28] and no-reference image based assesment metrics [27][29]. Table 4 and 5 displays the detailed scores of each algorithm in terms of the reference and no-reference image based assessment metrics respectively. The standard descriptor (i.e., mean±standard deviation) for each assessment metrics was used to characterize the quantitative performance. It can be observed from Table 3 that the methods proposed by S. Bhattacharya et.al. [14] and B. Li. et.al. [24] are the two best performing methods and comparative performs in terms of colour, texture, and structure information so as compared with the other state-of-the-art techniques. Conversely, the methods as proposed by Y. Li et.al. [15], D. Berman et.al. [19], and Y. Bahat et.al. [27] are the three worst performed methods and thereafter results in structural distortion of the scenes. Overall, all the used techniques achieve comparatively lower performance values in each of the assessment metrics and thus indicates the complexity of visibility enhancement techniques.

4. CONCLUSION

In this paper, a newly designed dataset entitled "SAMEER-TU Outdoor Dataset" is introduced in different atmospheric and weather degraded situations (i.e., fog, poor illumination, and clear scenes). Qualitative and quantitative analysis of the visibility enhancement techniques on our designed dataset reveals that the existing techniques are not ready to cope up with the fog situations (especially in dense fog situations) and leaves a significant gap for improvement both qualitatively and quantitatively.

5. ACKNOWLEDGEMENT

The work presented was supported by the Grant No. SMR/PD(R)/NER/2012-13/Thermography, Dated: 22nd March, 2013 from the Society for Applied Microwave Electronics Engineering and Research (SAMEER), Government of India. The first author is grateful to Council of Scientific and Industrial Research (CSIR), Government of India for providing the Senior Research Fellowship (SRF) under CSIR-SRF Fellowship Programme under Grant No. 09/714(0020)/2019-EMR-I, Dated: 01/04/2019.

6. REFERENCES

[1] B. Li, W. Ren, D. Fu, D. Tao, D. Feng, W. Zeng and Z. Wang, "Benchmarking single-image dehazing and beyond," *IEEE Transactions on Image Processing*, Vol. 28, No. 1, pp. 492-505, 2018.

[2] Y. Xu, J. Wen, L. Fei and Z. Zhang, "Review of video and image defogging algorithms and related studies on image restoration and enhancement," *IEEE Access*, Vol. 4, pp. 165-188, 2015.

[3] C.O. Ancuti, C. Ancuti and R. Timofte, "NH-HAZE: An Image Dehazing Benchmark with Non-Homogeneous Hazy and Haze-Free Images," *in Proc. IEEE/CVF Conference on Computer Vision and Pattern Recognition Workshops*, IEEE, pp. 444-445, 2020.

[4] C.O. Ancuti, C. Ancuti, R. Timofte and C.D. Vleeschouwer, "O-haze: a dehazing benchmark with real hazy and haze-free outdoor images," *in Proc. IEEE conference on computer vision and pattern recognition workshops*, IEEE, pp. 754-762, 2018.

[5] C.O. Ancuti, C. Ancuti, R. Timofte and C.D. Vleeschouwer, "I-HAZE: A dehazing benchmark with real hazy and haze-free indoor images," *arXiv 2018. arXiv preprint arXiv:1804.05091*, 2018.

[6] Y. Zhang, L. Ding and G. Sharma, "Hazerd: an outdoor scene dataset and benchmark for single image dehazing," *in Proc. 2017 IEEE international conference on image processing (ICIP)*, IEEE, pp. 3205-3209, 2017.

[7] C.O. Ancuti, C. Ancuti and C. D. Vleeschouwer, "D-hazy: A dataset to evaluate quantitatively dehazing algorithms," *in Proc. 2016 IEEE International Conference on Image Processing (ICIP)*, IEEE, pp. 2226-2230, 2016.

[8] J.P. Tarel, N. Hautiere, A. Cord, D. Gruyer and H. Halmaoui, "Improved visibility of road scene images under heterogeneous fog," *in Proc. 2010 IEEE Intelligent Vehicles Symposium*, IEEE, pp. 478-485, 2010.

[9] S.G. Narasimhan, C. Wang and S.K. Nayar, "All the images of an outdoor scene," *in Proc. European conference on computer vision*, Springer, Berlin, Heidelberg, pp. 148-162, 2002.

[10] S.G. Narasimhan and S.K. Nayar, "Vision and the atmosphere," *International Journal of Computer Vision*, Springer, Vol. 48, No. 3, pp. 233-254, 2002.

[11] SAMEER-TU Outdoor Dataset. [Online]. Available: http://www.mkbhowmik.in/sameer.aspx

[12] K. He, J. Sun, and X. Tang, "Single image haze removal using dark channel prior," *IEEE Transactions on Pattern Analysis and Machine Intelligence*, Vol. 33, No. 12, pp. 2341-2353, 2011.

[13] J.P. Tarel and N. Hautiere, "Fast visibility restoration from a single color or gray level image," *in Proc. 2009 IEEE 12th International Conference on Computer Vision*, IEEE, pp. 2201-2208, 2009.

[14] S. Bhattacharya, S. Gupta and K. S. Venkatesh, "Dehazing of color image using stochastic enhancement," *in Proc. 2016 IEEE International Conference on Image Processing*, IEEE, pp. 2251-2255, 2016.

[15] Y. Li, F. Guo, R.T. Tan and M.S. Brown, "A contrast enhancement framework with JPEG artifacts suppression," *in Proc. European Conference on Computer Vision*, Springer, pp. 174-188, 2014.

[16] Q. Zhu, J. Mai and L. Shao, "A fast single image haze removal algorithm using color attenuation prior," *IEEE Transactions on Image Processing*, Vol. 24, No. 11, pp. 3522-3533, 2015.

[17] G. Meng, Y. Wang, J. Duan, S. Xiang and C. Pan, "Efficient image dehazing with boundary constraint and contextual regularization," *in Proc. IEEE International Conference on Computer Vision*, pp. 617-624, 2013.

[18] W. Ren, S. Liu, H. Zhang, J. Pan, X. Cao and M.H. Yang, "Single image dehazing via multi-scale convolutional neural networks," *in Proc. European Conference on Computer Vision*, Springer, pp. 154-169, 2006.

[19] D. Berman and S. Avidan, "Non-local image dehazing," *in Proc. IEEE Conference on Computer Vision and Pattern Recognition*, IEEE, pp. 1674-1682, 2016.

[20] S.S. Colores, I.C. Aceves and J.M.R. Arreguin, "Single image dehazing using a multilayer perceptron," *Journal of Electronic Imaging*, SPIE, vol. 27, no. 4, pp. 043022, 2018.

[21] X. Fan, Y. Wang, X. Tang, R. Gao and Z. Luo, "Two-layer Gaussian process regression with example selection for image dehazing," *IEEE Transactions on Circuits and Systems for Video Technology*, Vol. 27, No. 12, pp. 2505-2517, 2017.

[22] B. Cai, X. Xu, K. Jia, C. Qing and D. Tao, "Dehazenet: An end-to-end system for single image haze removal," *IEEE Transactions on Image Processing*, Vol. 25, No. 11, pp. 5187-5198, 2016.

[23] G. Yadav, S. Maheshwari and A. Agarwal. "Foggy image enhancement using contrast limited adaptive histogram equalization of digitally filtered image: Performance improvement," *in Proc. 2014 International Conference on Advances in Computing, Communications and Informatics (ICACCI)*, IEEE, pp. 2225-2231, 2014.

[24] B. Li, X. Peng, Z. Wang, J. Xu and D. Feng, "Aod-net: All-in-one dehazing network," *in Proc. IEEE international conference on computer vision*, pp. 4770-4778, 2017.

[25] C.O. Ancuti and C. Ancuti, "Single image dehazing by multi-scale fusion," *IEEE Transactions on Image Processing*, Vol. 22, No. 8, pp. 3271-3282, 2013.

[26] C.O. Ancuti, C. Ancuti, C.D. Vleeschouwer and P. Bekaert, "Color balance and fusion for underwater image enhancement," *IEEE Transactions on Image Processing*, Vol. 27, No. 1, pp. 379-393, 2018.

[27] Y. Bahat and M. Irani, "Blind dehazing using internal patch recurrence," *in Proc. 2016 IEEE International Conference on Computational Photography*, IEEE, pp. 1-9, 2016.

[28] R. Sakuldee and S. Udomhunsakul, "Objective performance of compressed image quality assessments," *International Journal of Computer Science*, Vol. 2, No. 4, pp. 258-267, 2007.

[29] L.K. Choi, J. You and A.C. Bovik, "Referenceless prediction of perceptual fog density and perceptual image defogging," *IEEE Transactions on Image Processing*, Vol. 24, No. 11, 3888-3901, 2015.